molecular pharmaceutics

Article

Chemoproteomics Reveals the Anti-proliferative Potential of Parkinson's Disease Kinase Inhibitor LRRK2-IN-1 by Targeting PCNA Protein

Weichao Li, Yiqing Zhou, Guanghui Tang, Nai-Kei Wong, Mengquan Yang, Dan Tan, and Youli Xiao

Mol. Pharmaceutics, **Just Accepted Manuscript** • DOI: 10.1021/acs.molpharmaceut.8b00325 • Publication Date (Web): 11 Jul 2018

ACS Publications

is published by the American Chemical Society. 1155 Sixteenth Street N.W., Washington, DC 20036

Chemoproteomics Reveals the Anti-proliferative Potential of Parkinson's Disease Kinase Inhibitor LRRK2-IN-1 by Targeting PCNA Protein

Weichao Li,[1] Yiqing Zhou,[1] Guanghui Tang,[2] Nai-Kei Wong,[3] Mengquan Yang,[1,4] Dan Tan,[5] Youli Xiao[1,4,*]

[1]CAS Key Laboratory of Synthetic Biology, CAS Center for Excellence in Molecular Plant Sciences, Institute of Plant Physiology and Ecology, Shanghai Institutes for Biological Sciences, Chinese Academy of Sciences, Shanghai 200032, China. E-mail: ylxiao@sibs.ac.cn.

[2]School of Chemical Biology and Biotechnology, Peking University Shenzhen Graduate School, Shenzhen 518055, China

[3]State Key Discipline of Infection Diseases, Shenzhen Third People's Hospital, The Second Affiliated Hospital, Shenzhen University, Shenzhen 518112, China.

[4]University of Chinese Academy of Sciences, Beijing 100039, China

[5]Ruijin Hospital, Shanghai Jiaotong University School of Medicine, Shanghai 200025, China

* Corresponding author

Prof. Youli Xiao

CAS Key Laboratory of Synthetic Biology, CAS Center for Excellence in Molecular Plant Sciences, Institute of Plant Physiology and Ecology, Shanghai Institutes for Biological Sciences, Chinese Academy of Sciences, Shanghai 200032, China

Phone: 86-21-54924226

ylxiao@sibs.ac.cn

ABSTRACT

LRRK2-IN-1, one of the first selective inhibitors of leucine-rich repeat kinase 2 (LRRK2), was serendipitously found to exhibit potent anti-proliferative activity in several types of human cancer cells. In this study, we employed a chemoproteomic strategy utilizing a photoaffinity probe to identify the cellular target(s) of LRRK2-IN-1 underlying its anti-cancer activity. LRRK2-IN-1 was found to induce cell cycle arrest as well as cancer cell death through specifically binding to human PCNA (proliferating cell nuclear antigen) in cancer cells. Our current findings suggest the potential of LRRK2-IN-1 as a novel pharmacological molecule for scrutinizing cell physiology and furnish a logical foundation for the future development of therapeutic reagents for cancer.

KEYWORDS

LRRK2-IN-1; click chemistry; chemical proteomics; PCNA; anti-proliferative

INTRODUCTION

Parkinson's disease (PD) is a devastating neuronal degeneration disorder afflicting ~1% of people over 60 years of age worldwide.[1] Mutations and aberrant activity of leucine-rich repeat kinase 2 (LRRK2), a ~280 kDa multi-domain protein bearing serine/threonine kinase activity, have been suggested to play significant roles in PD,[2] galvanizing much interest in the discovery of LRRK2 inhibitors for the treatment of PD.[3-5] In 2011, significant progress was achieved in this field when LRRK2-IN-1 and CZC-25146 were established as potent and selective LRRK2 inhibitors (Fig. 1A).[6,7] However, while these inhibitors are "selective" within a finite kinome based on high-throughput screening with purified kinases in vitro, the specificity of these compounds across an extended scope of proteome (e.g., ADP/ATP-dependent protein interactome, or even the whole proteome) may vary considerably. For instance, glyoxalase-1, has been shown to be an off-target of CZC-25146 in HeLa cells.[8] Also, other pharmacological effects of LRRK2-IN-1 have been reported, including anti-cancer activity, ocular toxicity, and pro-inflammatory or immunomodulatory activity in neuro-inflammation.[9-11] While the primary mechanism of LRRK2-IN-1 have been extensively studied, the molecular target(s) responsible for its off-target effects, however, have remained elusive, which imposes a realistic obstacle to translational applications in medicine.

To tackle the above issues, we examined the anti-proliferative activity of LRRK2-IN-1 towards a series of human cancer cell lines, including Jurkat (lymphocyte), HeLa (cervical carcinoma), HCT116 (colon cancer), MCF-7 (breast cancer), and HepG2 (hepatocarcinoma). As shown in Figure 1B, LRRK2-IN-1 dose-dependently blunted the growth of these human cancer cells, with efficacy in low micromolar range in Jurkat cells. Cell cycle analysis revealed that LRRK2-IN-1 markedly increased the proportion of Jurkat cells in G_2/M phases (Figure 1C and Figure S4). Because no expression of LRRK2 was detected in Jurkat cells,[6] there might be additional functional target(s) of LRRK2-IN-1 in this cell line. Previously, LRRK2-IN-1 has been reported to elicit cell cycle arrest by suppressing DCLK1 kinase activity and inhibiting its mRNA and protein expression, which in turn inhibits downstream c-Myc signaling in colorectal and pancreatic cancer cells.[12] However, in human T lymphocyte Jurkat cells, we found LRRK2-IN-1 inhibits cell proliferation without affecting the expression of DCLK1 and c-Myc (Figure S5), suggesting the existence of additional target(s).

Recently, a number of research groups including us have reported the employment of chemical proteomics in target identification of bioactive small molecules.[13-16] In the present study, we combined A*f*BPP (affinity-based protein profiling) strategy with multiple molecule/cell-based experiments to identify the molecular targets as well as mode of actions of LRRK2-IN-1 in Jurkat cells. Proliferating cell nuclear antigen (PCNA), a processivity factor in cell replication, recruit proteins involved in chromatin remodeling, DNA repair, DNA replication, and epigenetics,[17] was identified as the potential off-target of LRRK2-IN-1. Interacting of PCNA by LRRK2-IN-1 offers a unifying mechanism to explain the anti-proliferative activities of LRRK2-IN-1, which could provide molecular basis for the development of related anti-cancer reagents.

EXPERIMENTAL METHODS

General Methods. All reagents used for the synthesis were purchased from TCI (Tokyo Kasei Kogyo, Inc), Sigma-Aldrich (St. Louis, USA), or MedChemExpress (Shanghai, China) and used without further purification. All recombinant proteins, enzymes, antibodies, and bio-reagents were purchased from Promega (Madison, USA), Life Technologies (Carlsbad, USA), Abcam (Cambridge, USA), Thermo Fisher Scientific (Waltham, USA), or Sangon (Shanghai, China). ^{1}H-NMR and ^{13}C-NMR spectra were recorded on a Bruker Advance ^{III} 500 (^{1}H: 500 MHz, ^{13}C: 125 MHz) with chemical shifts in ppm relative to residual D-chloroform (δ_H 7.26 and δ_C 77.16) as standard. HR-MS analyses were performed on a Waters Acquity UPLC tandem with a Q-Exactive™ mass spectrometer (Thermo Scientific). Confocal studies were performed using a laser scan microscopy Leica TCS SP8 STED 3X. Proteomic analyses were performed on a Thermo Orbitrap Fusion™ Lumos mass spectrometer (Thermo Scientific).

Kinase enzyme activity assay. The biochemical IC_{50} values of LRRK2-IN-1 and LK2-P1 against LRRK2 were measured by Invitrogen Adapta® assays. Data analyses were performed with GraphPad Prism 7.0.

Labeling of recombinant protein. Recombinant LRRK2 kinase (Merck, Inc.), PCNA (Abcam, Inc.), or BSA (Sangon Biotech) was diluted to 0.1 mg mL^{-1} in PBS. For inhibitor-competitive reactions pretreated with LRRK2-IN-1 (100 μM, 10×), MLi-2 (100 μM, 10×) or staurosporine (10 μM) for 30 min, then LK2-P1 (10 μM) was added as indicated for 30 min at on ice. Samples were transferred to 96-

well plate in a same line and irradiated with UV (365 nm, 8 Watt) on ice for 20 min. Each of 20 μL protein samples were added with 1% SDS and fresh prepared of Tetramethylrhodamine azide (TAMRA-N_3, 100 μM, Lumiprobe), $CuSO_4$ (1 mM, Sigma), Tris(3-hydroxypropyltriazolylmethyl)amine (THPTA, 100 μM, Sigma), and sodium ascorbate (1 mM). The samples were reacted at 37 ^oC for 1 hour, then separated by SDS-PAGE gel and detected by a FLA 9000 plus DAGE scanner (Fujifilm). Finally, the gel was visualized by Coomassie blue staining or silver staining.

Gel-based A*f*BPP in Jurkat cells. Jurkat cells were incubated respectively with probes or DMSO at 37 ^oC (for the enrichment experiment: the cells were treated with Dead-Dayne (10 μM) or LK2-P1 (10 μM), respectively for 3 hours; for the competitive experiment: the cells were treated with LRRK2-IN-1 (50 μM) used for competition or DMSO together with LK2-P1 (10 μM) for 3 hours at 37 ^oC) in 2.0 mL of fresh RPMI-1640 growth medium. After remove the growth medium, the cells then washed three times with ice-cold PBS, followed by irradiated by a UV lamp (365 nm, 8×3 watt) for 20 min. The cells were harvested by scraping the cells in ice-cold lysis buffer (50 mM HEPES, pH 8.0, 150 mM NaCl, 0.1% Triton X-100, 0.1 mM EDTA and cOmplete protease inhibitors). The lysed cells were centrifuged at 14,000 g for 5 min and the soluble fractions were adjusted to 2 mg mL^{-1} with lysis buffer containing 1% sodium dodecyl sulfate (SDS, w/v). Click reaction was performed in each sample as described above.

Mass spectrometry-based A*f*BPP. The probe incubation and proteome preparation procedures were same as that of labeling studies mentioned above. Each of 300 μL of proteome sample was mixed with biotin-N_3 (500 μM, Biomatrick Inc.), $CuSO_4$ (1 mM), THTPA (100 μM) and sodium ascorbate (1 mM) for 2 hours at 37 ^oC. The proteomes were then precipitated with adding $CH_3OH/CHCl_3/H_2O$: 4/1/2 (v/v) and vortexed for 5 min. After centrifuge at 14,000 g for 3 min, the protein disk was washed with CH_3OH (500 μL), air-dried and re-dissolved in 200 μL of 1% SDS in PBS. 50 μL of Streptavidin Sepharose High Performance affinity resin (GE Healthcare) were added to each sample and rotated gently at room temperature for 1 hour. Then the beads were washed sequentially with 1.0 % SDS in PBS three times, 0.5 M NaCl in PBS three times, 50 mM triethylammonium bicarbonate (TEAB) containing 4 M Urea two times, and 50 mM TEAB five times. All enriched proteins were subjected to on beads reduction with 5 mM of dithiothreitol (DTT, 250 μL) at 56 °C for 30 min and alkylation with

50 mM iodoacetamide (IAA, 250 μL) at 37 °C in dark for additional 30 min. Finally, the beads were washed three times with 100 mM of TEAB. Bound proteins then were digested by 0.5 μg of trypsin (Thermo Fisher) dissolved in 30 μL of 50 mM TEAB overnight at 37 °C. All digested peptides were reacted with TMT-sixplex^{TM} Isobaric Label Reagent (Thermo Scientific), based on the manufacturer's procedures, respectively (TMT^6-126 for DMSO treated sample; TMT^6-127 for Dead-Dayne treated sample; TMT^6-128 for LK2-P1 treated sample; TMT^6-128 for LK2-P1 and LRRK2-IN-1 treated sample). After desalted by Pierce C18 spin columns, the labeled peptides were diluted in 30 μL of acetonitrile/H_2O/formic acid (v:v:v = 5%/94.5%/0.5%). All pulldown experiments were performed in biological triplicates. A volume of 2 μL of peptides was loaded on a Acclaim PepMap100 column (5 μm, 0.3 mm × 5 mm) and eluted on an Acclaim PepMap RSLC column (30 μm × 10 cm).

Protein identification and quantification. ProteinGroups files were used for analysis using Perseus 1.5.1.6. For all files, proteins falling into the following categories were removed: identified only by site, reverse, contaminant. Data were matched to annotation data downloaded from Uniprot (http://www.uniprot.org/) in October, 2017 (proteome ID: UP000005640, total sequence 20230). The mass spectra raw data were analyzed by Proteome Discoverer 2.1 (Thermo Scientific). TMT-sixplex (Lys and N-terminal) and carbamidomethyl (Cys, +57.0215 Da) were used as static modifications, oxidation (Met, +15.9949 Da) was used as a variable modification. Protein ratios were calculated as the median of all peptide hits belonging to a certain protein. Statistical analysis was performed with Perseus. TMT ratios obtained from Proteome Discoverer 2.1 were transformed by $\log_2(x)$, normalized using Z-score, $-\log_{10}(p\text{-value})$ were obtained by a two sided one sample t-test over three biological replicates. Proteins were ranked according to the sum of the ranking values from TMT ratios and $-\log_{10}(p\text{-value})$ across both experiments (enrichment experiment: LK2-P1/Dead-Dayne, competition experiment: LK2-P1/LK2-P1+LRRK2-IN-1). Only proteins identified have ratios higher than 4.0 and *p*-values less than 0.05 were considered as statistical significant targets.

Binding site identification. 1 μg of recombinant PCNA protein (Abcam, Inc.) in PBS (20 μL) were incubated with 10 μM of LK2-P1 at 0 ^{o}C for 1 hour, followed by irradiated by a UV lamp (365 nm, 8×3 watt) for 20 min. After SDS-PAGE gel separation and reductive alkylation, 0.5 μg of trypsin (Thermo Scientific) was added and the sample was incubated at 37 °C overnight. The digests were desalted by Ziptip desalting column (Pierce), dried on a SpeedVac. The dried peptides were diluted in

20 μL of acetonitrile/H_2O/formic acid (v:v:v = 5%/94.5%/0.5%) with sonication and analyzed by Thermo Orbitrap Fusion™ Lumos proteomic mass spectrometer as mentioned above. The mass spectra data was analyzed by Proteome Discoverer 2.1 (Thermo Scientific). The database used was the protein sequence of human PCNA (UniprotKB ID: P12004, sequence download date: June, 2017). The search parameters used were as follows: Trypsin Digestion; carbamidomethyl (Cys, +57.0215 Da), oxidation (Met, +15.9949 Da), LK2-P1 probe modified residue mass difference 567.29 amu was specified as variable modification at serine, valine, glycine, arginine, isoleucine, proline, tryptophan, leucine, phenylalanine, methionine, cysteine, glutamic acid, tyrosine, lysine, histidine, threonine, alanine and aspartic acid residues. Fragment Mass Tolerance was 0.02 Da, Peptide Mass Tolerance was 10 ppm and target false discovery rate (FDR) was 1%. Manual verification was performed to ensure confident peptide identification

RESULT AND DISCUSSION

First, a LRRK2-IN-1-derived photoaffinity probe, LK2-P1 (Figure 2A) was synthesized by tagging a minimal-sized diazirine-containing clickable handle to the scaffold (Scheme 1).[18] Dead-Dayne, a negative control probe, was employed to exclude potential non-specific binding proteins.[19] *In vitro* kinase assays showed LK2-P1 exhibited comparable activity towards LRRK2 as its parent compound (Figure 2B). Next, we examined the labeling efficiency of LK2-P1 on recombinant LRRK2 proteins. Competition experiment showed that the labeling was indeed activity-based (Figure 2C). Then, we carried out cell-based assays to examine the anti-proliferative activity of the probe. LK2-P1 inhibited the growth of Jurkat cells with efficacy similar to that of LRRK2-IN-1 (Figure S6), and also caused cell cycle arrest in the G_2/M phase (Figure S4). Collectively, these results demonstrate that LK2-P1 is indeed a cell-permeable probe that sufficiently retains LRRK2-IN-1 activity for exploring potential binding proteins in living cells.

In order to detect the binding protein(s) of LRRK2-IN-1, we performed gel-based labelling experiments in living Jurkat cells. Cells were incubated with LK2-P1 (10 μM) in the presence or absence of excess LRRK2-IN-1 (50 μM, 5-fold) as a competitor. To discriminate background proteins of diazirine-alkyne moiety, an identically designed experiment was added with the control probe Dead-Dayne (10 μM). After probe incubation and photocrosslinking, Jurkat cells were lysed. The samples

were coupling to TAMRA-N_3 *via* click chemistry and analyzed by SDS-PAGE gel-based fluorescence (Figure 3A and Figure S7). Proteins of the size around 35 kDa were labelled predominately (lane 2), with most of these labelled proteins being able to be abolished with excess LRRK2-IN-1 (lane 3). Probe labelling of virtually all detected proteins was UV-dependent and few proteins showed up as photocrosslinker-binders (lanes 1 and 2). Furthermore, intracellular click reaction was applied to visualize the subcellular localization of LK2-P1. LK2-P1- or Dead-Dayne- (both 10 μM) treated cells. After UV-crosslinked, fixed and permeabilized, Jurkat cells were conjugated to TAMRA-N_3. In LK2-P1-treated cells, fluorescent signals were observed in both the nucleus and cytoplasm, while few signals were observed in Dead-Dayne-treated cells, suggesting the fluorescence represented proteins labeled by LK2-P1 (Figure 3B).

To identify the cellular targets of LK2-P1, we next performed large-scale pull-down/LC-MS experiments by quantitative proteomics. Probe-labelled proteomes prepared same as those in gel-based experiments were conjugated with biotin-N_3 and enriched by pull-down with streptavidin sepharose affinity resin. Enriched proteins were processed for on beads tryptic digestion and the digestion products were labelled with tandem mass tag (TMT) reagents, respectively, followed by mass spectra analysis. The proteomics experiment was carried out in biological triplicates. To reduce false-positives, identified proteins were ranked in the corresponding volcano plots as a ($\log_2$) of enrichment ratio (LK2-P1 versus Dead-Dayne) as well as competition ratio (LK2-P1 versus LK2-P1 + LRRK2-IN-1) against statistical significance ($\log_{10}$ *p*-value). Proteins enriched or competed by a factor > 4 with *p*-value < 0.05 were considered hits (Figure 4A, 4B and Tables S1, S2). As shown in Figure 4A and 4B, proliferating cell nuclear antigen (PCNA), a nuclear protein plays significant roles in DNA synthesis and cell proliferation, especially in cancerous cells, was identified as the most significant hit in both enrichment and competition experiments.[17] Similar proteomics experiments were repeated in HeLa cells, as shown in Figure S8, PCNA also significantly targeted, confirms PNCA as the off-target of LRRK2-IN-1 (Tables S3, S4)。 In-gel competitive photo-labelling experiments provided evidence that PCNA was specially labelled in both UV- and LRRK2-IN-1-dependent manners (Figure 4C). Enrichment of PCNA was also confirmed by competition pulldown and immunoblotting experiments as previously described (Figure 4D). Furthermore, to assess whether PCNA is engaged by LRRK2-IN-1 in living cells, a cellular thermal-shift assay (CETSA) was also performed to compared the thermal stability of PCNA between

drug- and DMSO-treated Jurkat cells.[20] PCNA was significantly stabilized upon drug treatment in situ with ΔTm of 6.7 °C, as indicated by a significant temperature increase required for protein loss by precipitation compared to DMSO controls (Figure 4E). Collectively, these results confirmed PCNA as a specific LRRK2-IN-1 binding protein.

Structurally, three monomers of PCNA configured as a hexagonal structure, form a molecular sliding clamp around the DNA double helix.[17] The interior of the clamp interacts with DNA, while the outer surface of the clamp contains an interdomain connector loop (IDCL), which was a binding area of many PCNA-interacting proteins.[21] To investigate the binding site of LK2-P1, recombinant PCNA proteins photo-labelled with LK2-P1 was digested and analyzed by mass spectra.[22] The peptide ^{218}ATPLSSTVTLSMSADVPLVVEYK^{240} was found to be covalently modified by the probe whose molecular weight increased by an expected increment (567.29 Da, LK2-P1 with loss of N_2) relative to the unmodified peptide fragment. Further analysis of the MS2 spectrum of this peptide localized the labelling on the side chain carboxyl group of Glu238 (Figure 5A and Figure S9). Based on the identified binding site, we then performed molecular docking studies to elucidate the interaction at atomic level. As shown in Figure 5B and Figure S10, the aminopyrimidine scaffold of LRRK2-IN-1 is in close proximity of the IDCL domain (residues Glu124-Ile128), a key region responsible for interacting with binding proteins.[23] As a key modulator of DNA synthesis, PCNA specifically binds with two DNA polymerases, namely DNA polymerases δ (Pol δ) and ε (Pol ε), to regulate DNA replication and repair in eukaryotes.[17, 23-24] Therefore, we speculated that LRRK2-IN-1-complexed PCNA becomes relatively insensitive to the DNA polymerases binding, resulting in the reduction of DNA replication and synthesis. To verify the hypothesis, proteins immunoprecipitated by antibody of PCNA from both LRRK2-IN-1- and Dead-Dayne-treated Jurkat cells were subjected to immunoblot analysis by using respective antibodies. Both DNA polymerases in LRRK2-IN-1-treated cells showed a weakened binding affinity to PCNA (Figure 5C), suggesting that LRRK2-IN-1 did disrupt the binding between PCNA and DNA polymerases δ and ε. Because disruption of PCNA-DNA polymerases interaction has been reported to cause the inhibition of DNA synthesis and hence cell apoptosis,[25-27] we thus examined the level of DNA synthesis upon LRRK2-IN-1 treatment by 5-ethynyl-2'-deoxyuridine (EdU) incorporation assay.[28] T2AA, a known PCNA inhibitor, was tested in parallel as positive control.[26] As shown in Figure 5D, incorporation of EdU was dose-dependently inhibited by LRRK2-IN-1 and T2AA with IC_{50}

values of 0.26 μM and 1.63 μM, respectively, validating our discovery. Furthermore, We utilized short hairpin RNA (shRNA)-based knockdown of PCNA to validate its roles in LRRK2-IN-1-mediated inhibition of cell proliferation as previously reported.[29] Knockdown of PCNA was confirmed by Western blot (Figure 5E), and resulted in an obvious cell cycle arrest in G_2/M phase (Figure 5F) which was similar to that of known small molecules PCNA inhibitors, such as p21 and PCNA-I1.[27,30] Taken together, these results further confirmed LRRK2-IN-1 exhibits its anti-proliferative activity through binding PCNA and acting as a protein-protein interaction (PPI) inhibitor of PCNA in Jurkat cells, linking PCNA binding with phenotypic response. MLi-2, a well-known potent and highly selective LRRK2 inhibitor, was used in parallel as validated negative control.[34] Both in Gel-based competitive labelling experiment and cell proliferation assay, MLi-2 did not shown the similar activity in comparisons with LRRK2-IN-1 (Figure S11). Together these data strongly link PCNA to the cell proliferation inhibition response to LRRK2-IN-1.

CONCLUSION

So far, diaminopyrimidine scaffold agents have been extensively applied in medicine chemistry.[31,32] However, the high frequency of off-target activity of small molecules could lead to unanticipated outcomes in drug development programs which seriously hindered the development of this field.[33] In the present study, we reported the first proteome-wide profiling of LRRK2-IN-1 in living cancer cells by using a cell-permeable photoaffinity probe, LK2-P1. With LK2-P1, PCNA was identified as a potential off-target of LRRK2-IN-1 in Jurkat cells. Accordingly, we carried out multiple molecule/cell-based experiments to validate PCNA as a specific target of LRRK2-IN-1. We demonstrated that LRRK2-IN-1 specifically binds PCNA and prevents it from interacting with DNA polymerases, which reveals a novel mechanism for the anti-proliferative activity of LRRK2-IN-1. Regardless additional off-targets that could escape the examination with the A*f*BPP strategy, this work emphasize the unique inhibitory effect of PCNA on the cell proliferation inhibition of LRRK2-IN-1. These results should furnish a logical foundation for the future design and development of related kinase inhibitors as well as anti-cancer agents.

ASSOCIATED CONTENT

Supporting Information

The Supporting Information is available free of charge on the ACS Publications website at DOI: 10.1021/acsmolpharmaceut.xxx.

Additional details of experiments and material characterization including the synthetic method of **LK-P1**, biological experimental details, and quantitative proteomic analyze detail lists (PDF).

AUTHOR INFORMATION

Corresponding Author

* E-mail: ylxiao@sibs.ac.cn. Tel: +86-21-54924226.

ORCID

Weichao Li: 0000-0001-6875-7315

Yiqing Zhou: 0000-0002-6391-3259

Mengquan Yang: 0000-0001-6473-1409

Youli Xiao: 0000-0002-4803-3333

Notes

The authors declare no competing financial interests.

ACKNOWLEDGMENTS

This work was supported by grants including XDPB0402 of CAS, NSFC 21572243 and 21502206. We thank X. Deng from Xiamen University for valuable discussion, and staff members (Y. Liu, Y. Shan, Y. He, and S. Bu) in the Core Facility Centre of the Institute of Plant Physiology and Ecology for technical assistance in mass spectrometry, confocal imaging and NMR. We also thank Y. Tao from IHS, CAS for kind support in cell experiments.

REFERENCES

(1) Nussbaum, R.; Ellis, C. Alzheimer's disease and Parkinson's disease. *N. Engl. J. Med.* **2003**, *348* (14), 1356-1364.

(2) Gilks, W.; Abou-Sleiman, P.; Gandhi, S.; Jain, S.; Singleton, A.; Lees, A.; Shaw, K.; Bhatia, K.; Bonifati, V.; Quinn, N.; Lynch, J.; Healy, D.; Holton, J.; Revesz, T.; Wood, N. A common LRRK2 mutation in idiopathic Parkinson's disease. *Lancet* **2005**, *365* (9457), 415-416.

(3) Zhang, J.; Deng, X.; Choi, H. G.; Alessi, D. R.; Gray, N. S. Characterization of TAE684 as a potent LRRK2 kinase inhibitor. *Bioorg. Med. Chem. Lett.* **2012**, *22* (5)**,** 1864–1869.

(4) Choi, H.; Zhang, J.; Deng, X.; Hatcher, J.; Patricelli, M.; Zhao, Z.; Alessi, D.; Gray, N. S. Brain penetrant LRRK2 inhibitor. *ACS Med. Chem. Lett.* **2012**, *3* (8), 658–662.

(5) Estrada, A.; Liu, X.; Baker-Glenn, C.; Beresford, A.; Burdick, D.; Chambers, M.; Chan, B. K.; Chen, H.; Ding, X.; DiPasquale A. G.; Dominguez, S. L. "Discovery of highly potent, selective, and brain-penetrable leucine-rich repeat kinase 2 (LRRK2) small molecule inhibitors. *J. Med. Chem.* **2012**, *55* (22), 9416–9433.

(6) Ramsden, N.; Perrin, J.; Ren, Z.; Lee, B. D.; Zinn, N.; Dawson, V. L.; Tam, D.; Bova, M.; Lang, M.; Drewes, G.; Bantscheff, M. Chemoproteomics-based design of potent LRRK2-selective lead compounds that attenuate Parkinson's disease-related toxicity in human neurons. *ACS Chem. Biol*. **2011**, *6* (10), 1021-1028.

(7) Deng, X.; Dzamko, N.; Prescott, A.; Davies, P.; Liu, Q.; Yang, Q.; Lee, J. D.; Patricelli, M. P.; Nomanbhoy, T. K.; Alessi, D. R.; Gray, N. S. Characterization of a selective inhibitor of the Parkinson's disease kinase LRRK2. *Nat. Chem. Biol.* **2011**, *7* (4), 203-205.

(8) Zhou, Y.; Guo, T.; Li, X.; Dong, Y.; Galatsis, P.; Johnson, D. S.; Pan, Z. Discovery of selective 2, 4-diaminopyrimidine-based photoaffinity probes for glyoxalase. *MedChemComm*. **2014**, *5* (3), 352-357.

(9) Luerman, G. C.; Nguyen, C.; Samaroo, H.; Loos, P.; Xi, H.; Hurtado□Lorenzo, A.; Needle, E.; Stephen Noell, G.; Galatsis, P.; Dunlop, J.; Geoghegan, K. F. Phosphoproteomic evaluation of pharmacological inhibition of leucine-rich repeat kinase 2 reveals significant off-target effects of LRRK2-IN-1. *J. Neurosci.* **2014**, *128* (4), 561-576.

(10) West, R. J.; Furmston, R.; Williams, C. A.; Elliott, C. J. Neurophysiology of Drosophila models of Parkinson's disease. *Parkinson's Dis.* **2015**, *2015*, 11.

(11) Russo, I.; Berti, G.; Plotegher, N.; Bernardo, G.; Filograna, R.; Bubacco, L.; Greggio, E. Leucine-rich repeat kinase 2 positively regulates inflammation and down-regulates NF-κB p50 signaling in cultured microglia cells. *J. Neuroinflammation* **2015**, *12* (1), 230.

(12) Weygant, N.; Qu, D.; Berry, W. L.; May, R.; Chandrakesan, P.; Owen, D. B.; Sureban, S. M.; Ali, N.; Janknecht, R.; Houchen, C. W. Small molecule kinase inhibitor LRRK2-IN-1 demonstrates potent activity against colorectal and pancreatic cancer through inhibition of doublecortin-like kinase 1. *Mol. Cancer* **2014**, *13* (1), 103.

(13) Lehmann, J.; Wright, M.; Sieber, S. Making a long journey short: alkyne functionalization of natural product scaffolds. *Chem.-Eur. J.* **2016**, *22* (14), 4666-4678.

(14) Zhu, B.; Zhang, H.; Pan, S.; Wang, C.; Ge, J.; Lee, J.; Yao, S. In situ proteome profiling and bioimaging applications of small-molecule affinity-based probes derived from DOT1L inhibitors. *Chem.-Eur. J.* **2016**, *22* (23), 7824-7836.

(15) Lehmann, J.; Richers, J.; Pöthig, A.; Sieber, S. Synthesis of ramariolide natural products and discovery of their targets in mycobacteria. *Chem. Commun.* **2017**, *53* (1), 107-110.

(16) Zhou, Y.; Li, W.; Zhang, X.; Zhang, H.; Xiao, Y. Global profiling of cellular targets of gambogic acid by quantitative chemical proteomics. *Chem. Commun.* **2016**, *52 (97)*, 14035-14038.

(17) Moldovan, G.; Pfander, B.; Jentsch, S. PCNA, the maestro of the replication fork. *Cell* **2007**, *129* (4), 665-679.

(18) Li, Z.; Hao, P.; Li, L.; Tan, C. Y.; Cheng, X.; Chen, G.; Sze, S.; Shen, H.; Yao, S. Design and synthesis of minimalist terminal alkyne□containing diazirine photo□crosslinkers and their incorporation into kinase inhibitors for cell□and tissue□based proteome profiling. *Angew. Chem. Int. Ed. Engl.* **2013**, *52* (33), 8551-8556.

(19) Zhou, Y.; Di, Z.; Li, X.; Shan, Y.; Li, W.; Zhang, H.; Xiao, Y. Chemical proteomics reveal CD147 as a functional target of pseudolaric acid B in human cancer cells. *Chem. Commun.* **2017**, *53* (62), 8671-8674.

(20) Jafari, R.; Almqvist, H.; Axelsson, H.; Ignatushchenko, M.; Lundbäck, T.; Nordlund, P.; Molina, D. M. The cellular thermal shift assay for evaluating drug target interactions in cells. *Nat. Protoc.* **2014**, *9* (9), 2100-2122.

(21) Kelman, Z. PCNA: structure, functions and interactions. *Oncogene* **1997**, *14* (6), 629–640.

(22) Li, W.; Zhou, Y.; Tang, G.; Xiao, Y. Characterization of the artemisinin binding site for translationally controlled tumor protein (TCTP) by bioorthogonal click chemistry. *Bioconjugate Chem.* **2017**, *27* (12), 2828-2833.

(23) Bravo, R.; Frank, R.; Blundell, P.; Macdonald-Bravo, H. Cyclin/PCNA is the auxiliary protein of DNA polymerase-δ. *Nature* **1987**, *326* (6112), 515–517.

(24) Shivji, M.; Kenny, M.; Wood, R. Proliferating cell nuclear antigen is required for DNA excision repair. *Cell* **1992**, *69* (2), 367-374.

(25) Inoue, A.; Kikuchi, S.; Hishiki, A.; Shao, Y.; Heath, R.; Evison, B.; Actis, M.; Canman, C.; Hashimoto, H.; Fujii, N. A small molecule inhibitor of monoubiquitinated Proliferating Cell Nuclear Antigen (PCNA) inhibits repair of interstrand DNA cross-link, enhances DNA double strand break, and sensitizes cancer cells to cisplatin. *J. Biol. Chem.* **2014**, *289* (10), 7109-7120.

(26) Punchihewa, C.; Inoue, A.; Hishiki, A.; Fujikawa, Y.; Connelly, M.; Evison, B.; Shao, Y.; Heath, R.; Kuraoka, I.; Rodrigues, P.; Hashimoto, H.; Kawanishi, M.; Sato, M.; Yagi, T.; Fujii, N. Identification of small molecule proliferating cell nuclear antigen (PCNA) inhibitor that disrupts interactions with PIP-box proteins and inhibits DNA replication. *J. Biol. Chem.* **2012**, *287* (17), 14289-14300.

(27) Tan, Z.; Wortman, M.; Dillehay, K.; Seibel, W.; Evelyn, C.; Smith, S.; Malkas, L.; Zheng, Y.; Lu, S.; Dong, Z. Small-molecule targeting of proliferating cell nuclear antigen chromatin association inhibits tumor cell growth. *Mol. Pharmacol.* **2012**, *81* (6), 811-819.

(28) Porro, A.; Berti, M.; Pizzolato, J.; Bologna, S.; Kaden, S.; Saxer, A.; Ma, Y.; Nagasawa, K.; Sartori, A.; Jiricny, J. FAN1 interaction with ubiquitylated PCNA alleviates replication stress and preserves genomic integrity independently of BRCA2. *Nat. Commun.* **2017**, *8* (1), 1073-1087.

(29) Ghosal, G.; Leung, J.; Nair, B.; Fong, K.; Chen, J. Proliferating cell nuclear antigen (PCNA)-binding protein C1orf124 is a regulator of translesion synthesis. *J. Biol. Chem.* **2012**, *287* (41), 34225-34233.

(30) Li, R.; Waga, S.; Hannon, G.; Beach, D.; Stillman, B. Differential effects by the p21 CDK inhibitor on PCNA-dependent DNA replication and repair. *Nature* **1994**, *371* (6497), 534-537.

(31) Miduturu, C.; Deng, X.; Kwiatkowski, N.; Yang, W.; Brault, L.; Filippakopoulos, P.; Chung, E.; Yang, Q.; Schwaller, J.; Knapp, S.; King, R.; Lee, J.; Herrgard, S.; Zarrinkar, P.; Gray, N.

High-throughput kinase profiling: a more efficient approach toward the discovery of new kinase inhibitors. *Chem. Biol.* **2011**, *18* (7), 868-879.

(32) Rudolph, U.; Knoflach, F. Beyond classical benzodiazepines: novel therapeutic potential of GABA A receptor subtypes. *Nat. Rev. Drug Discov.* **2011**, *10* (9), 685-697.

(33) Campillos, M.; Kuhn, M.; Gavin, A.; Jensen, L.; Pork, P. Drug target identification using side-effect similarity. *Science* **2008**, *321* (5886), 263-266.

(34) Fell, M. J.; Mirescu, C.; Basu, K.; Cheewatrakoolpong, B.; DeMong, D. E.; Ellis, J. M.; Hyde, L. A.; Lin, Y.; Markgraf, C. G.; Mei, H.; Miller, M.; Poulet, F. M.; Scott, J. D.; Smith, M. D.; Yin, Z.; Zhou, X.; Parker, E.; Kennedy, M. E.; Morrow, J. A. MLi-2, a potent, selective, and centrally active compound for exploring the therapeutic potential and safety of LRRK2 kinase inhibition. *J. Pharmacol. Exp. Ther.* **2015**, *355* (3), 397-409.

FIGURE LEGENDS

Figure 1. (A) Structure of LRRK2-IN-1. (B) Cell proliferation assays of LRRK2-IN-1 against human cancer cell lines. (C) Cell cycle analysis in Jurkat cells after LRRK2-IN-1 (10 μM) treatment, demonstrating robust G_2/M arrest.

Figure 2. LRRK2-IN-1 based photo-affinity probe. (A) Structure of LK2-P1 and Dead-Dayne. (B) Dose-dependent inhibition of LRRK2 by LRRK2-IN-1, LK2-P1 and Dead-Dayne. Values represent the means ± S.D. of duplicates in two independent experiments. (C) Profiles for competition of LK2-P1 labelling with LRRK2-IN-1 (LKI) and staurosporine (STA, a pan-kinase inhibitor). Probe-labelled proteins were visualized by click conjugation to the TAMRA-azide tag, SDS gel separation, and fluorescence scanning. The concentration used for LK2-P1 in labeling experiments was 10 μM.

Figure 3. Fluorescence labeling of LK2-P1 in Jurkat cells. (A) Gel-based profiling of LK2-P1 labelled in intact Jurkat cells. (B) Confocal fluorescence imaging of Jurkat cells. The cells were treated with LK2-P1, irradiated by UV light as indicated, conjugated with TAMRA-N_3 (red) and stained with the nuclear DNA dye DAPI (4,6-diamidino-2-phenylindole, blue) (BF, bright field).

Figure 4. Chemoproteomics profiling of LRRK2-IN-1 in Jurkat cells. (A, B) Quantitative mass spectrometry-based profiling of LRRK2-IN-1 binding proteins in intact Jurkat cells. Green and red dots depict selected targets that are outcompeted by Dead-Dayne (A) or LRRK2-IN-1 (B) (criteria: $\log_2$-fold enrichment ≥ 2 and $-\log_{10}(p\text{-value}) \geq 1.33$). (C) Competition of LK2-P1 (10 μM) labeling recombinant PCNA (lanes 1-3) and BSA (lanes 4-6), LRRK2-IN-1 at a concentration 5 folds that of LK2-P1. (D) Preliminary validation of PCNA by PD/WB from LK2-P1 (10 μM)-labelled Jurkat lysates. The corresponding control experiments were done with DMSO, the negative probe (Dead-Dayne) and LRRK2-IN-1 at a concentration 5 folds that of LK2-P1 (10×LRRK2-IN-1). (E) Cellular thermal-shift assay (CETSA). Stabilization of PCNA after incubating cells with LRRK2-IN-1/DMSO, respectively. The band intensity of soluble PCNA at 47 ^{o}C is set at 100%, the band intensity of the remaining soluble protein at different temperatures were measured, the data were fitted to obtain apparent ΔT_m values using the Boltzmann Sigmoid equation within GraphPad Prism 7.0.

Figure 5. Validation of PCNA as an off-target of LRRK2-IN-1. (A) MS2 spectrum of LK2-P1-modified peptide with PCNA protein, (LK2, LK2-P1; O, Oxidation). (B) Docking of LRRK2-IN-1 into the PIP-box of PCNA (PDB ID code: 3WGW). (C) DNA polymerase δ and ε could not be co-immunoprecipitated with PCNA after LRRK2-IN-1 treatment

in Jurkat cells. (D) Effects of LRRK2-IN-1 and T2AA on DNA replication in Jurkat cells. The EdU incorporation and dose dependence of drug treatment were quantified by fluorescent microplate reader. (E) Validation of PCNA knockdown by Western blot analysis. Cells treated with scrambled shRNA served as a negative control (Scr). (F) Jurkat cells were transfected with Sh-Scr or Sh-PCNA, and analysed *via* flow cytometry after 24 h.

FIGURES

Figure 1

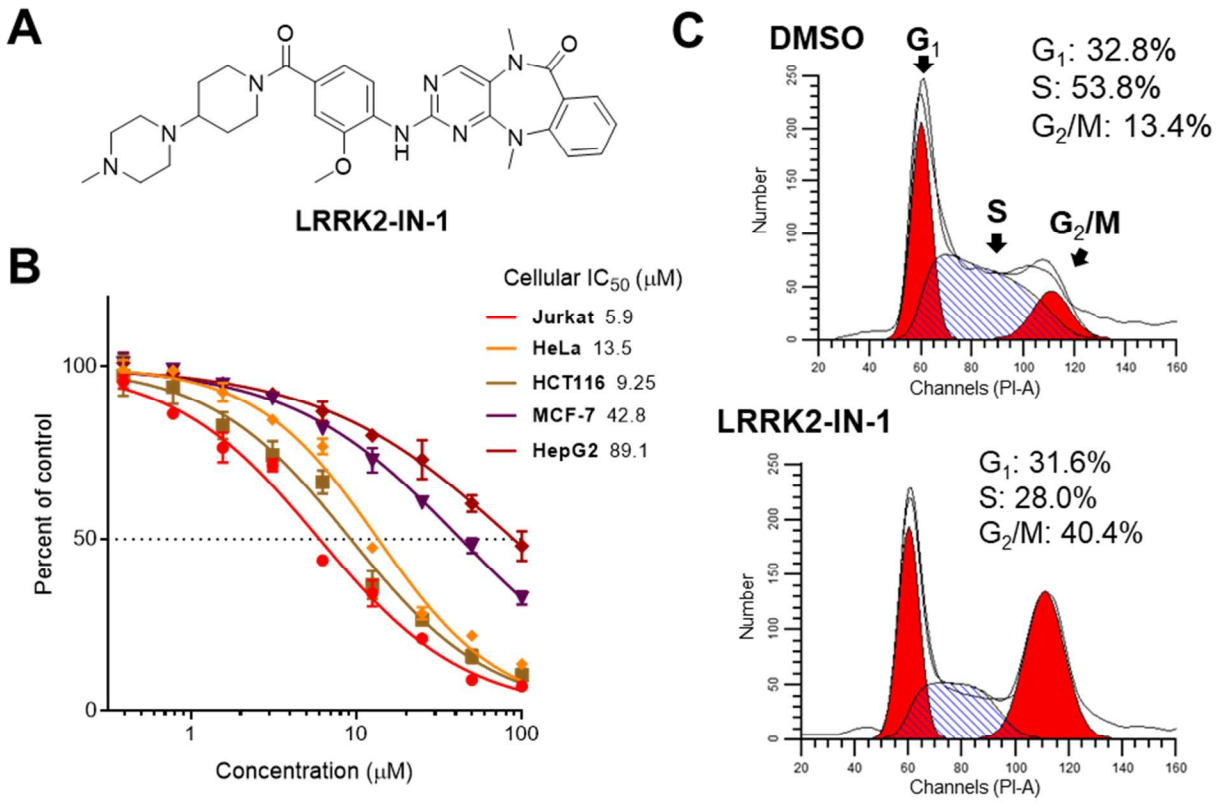

Figure 2

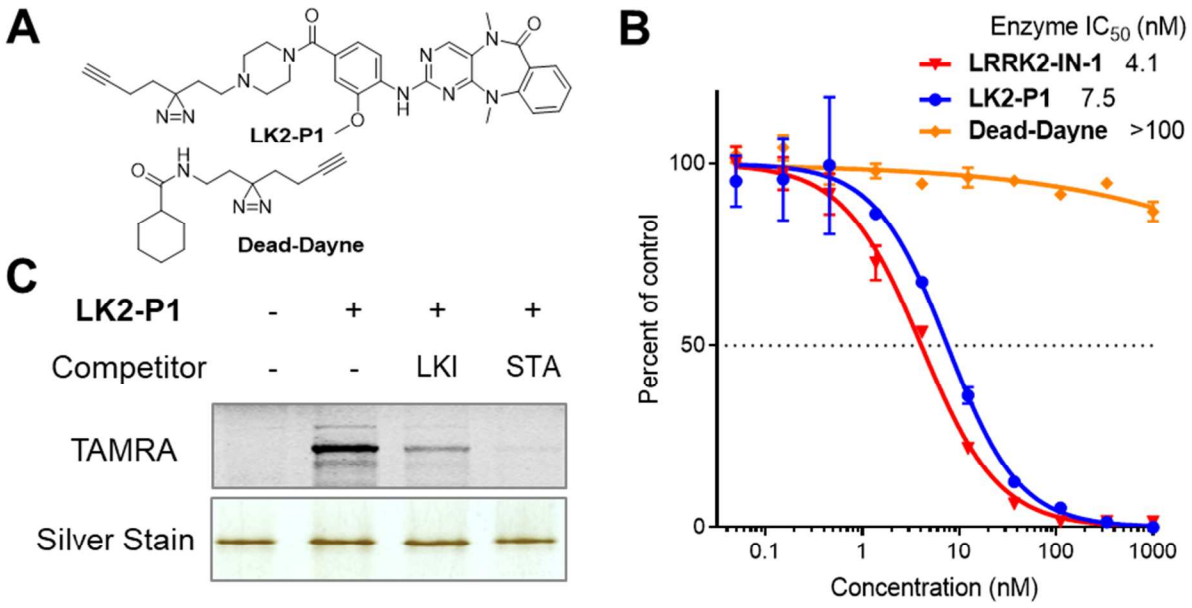
A
LK2-P1
Dead-Dayne
B
Enzyme IC50 (nM)
LRRK2-IN-1 4.1
LK2-P1 7.5
Dead-Dayne >100
Percent of control
100
50
0
0.1
1
10
100
1000
Concentration (nM)
C
LK2-P1 - + + +
Competitor - - LKI STA
TAMRA
Silver Stain

Figure 3

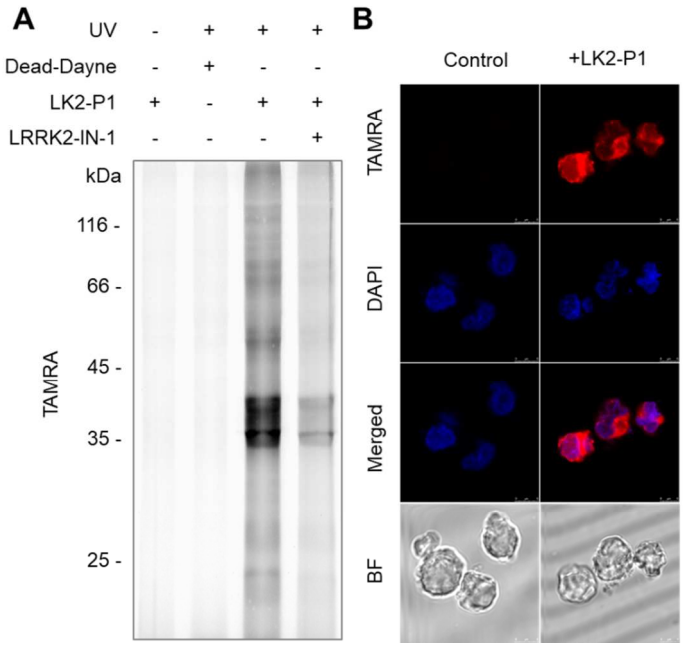
A
UV - + + +
Dead-Dayne - + - -
LK2-P1 + - + +
LRRK2-IN-1 - - - +
kDa
116 -
66 -
45 -
35 -
25 -
TAMRA
B
Control
+LK2-P1
TAMRA
DAPI
Merged
BF

Figure 4

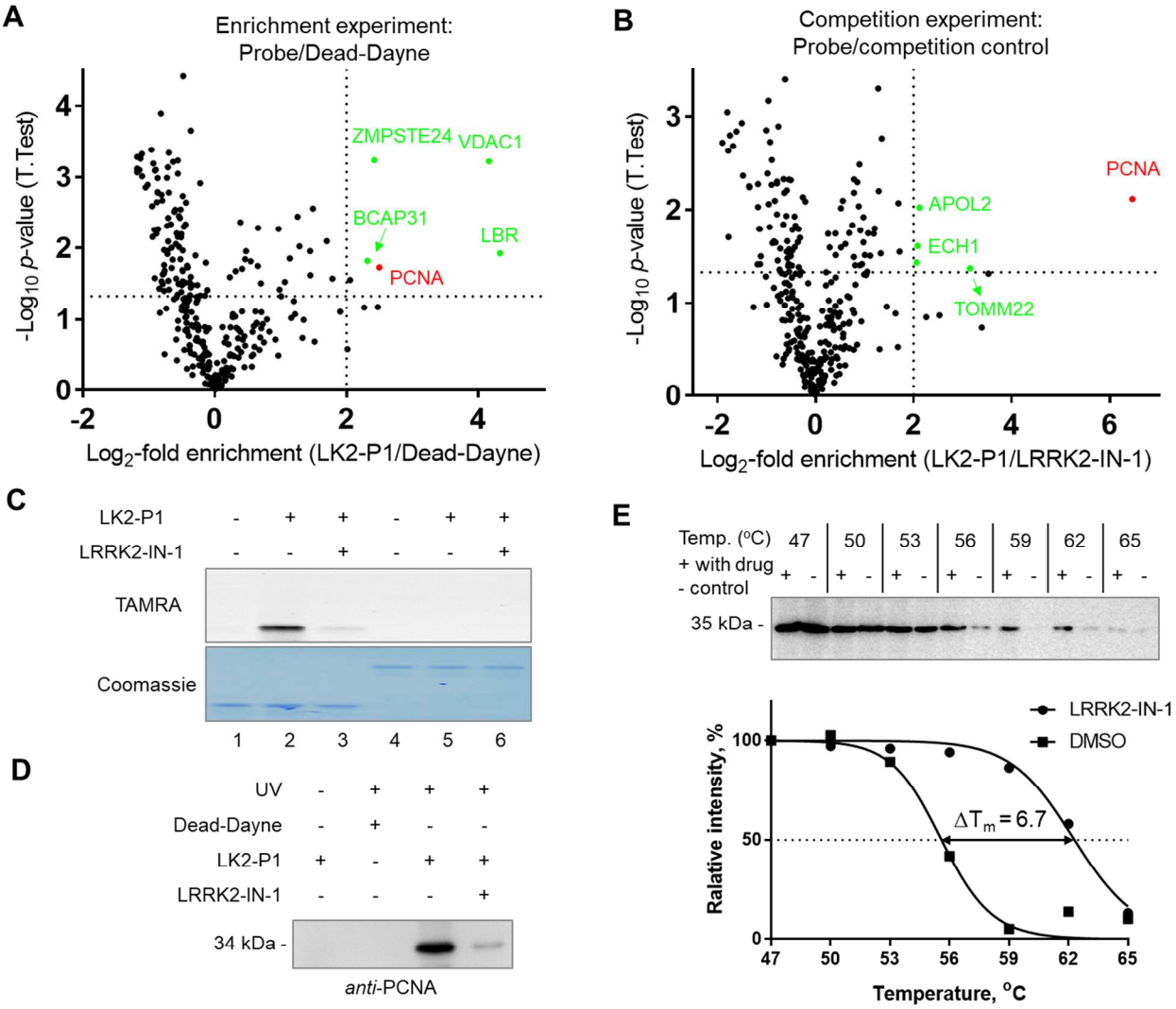
A
Enrichment experiment:
Probe/Dead-Dayne
-Log10 p-value (T.Test)
Log2-fold enrichment (LK2-P1/Dead-Dayne)
ZMPSTE24
VDAC1
BCAP31
LBR
PCNA
B
Competition experiment:
Probe/competition control
-Log10 p-value (T.Test)
Log2-fold enrichment (LK2-P1/LRRK2-IN-1)
PCNA
APOL2
ECH1
TOMM22
C
LK2-P1
LRRK2-IN-1
TAMRA
Coomassie
1 2 3 4 5 6
D
UV
Dead-Dayne
LK2-P1
LRRK2-IN-1
34 kDa
anti-PCNA
E
Temp. (°C) 47 50 53 56 59 62 65
+ with drug
- control
35 kDa
LRRK2-IN-1
DMSO
Ralative intensity, %
ΔTm = 6.7
Temperature, °C

Figure 5

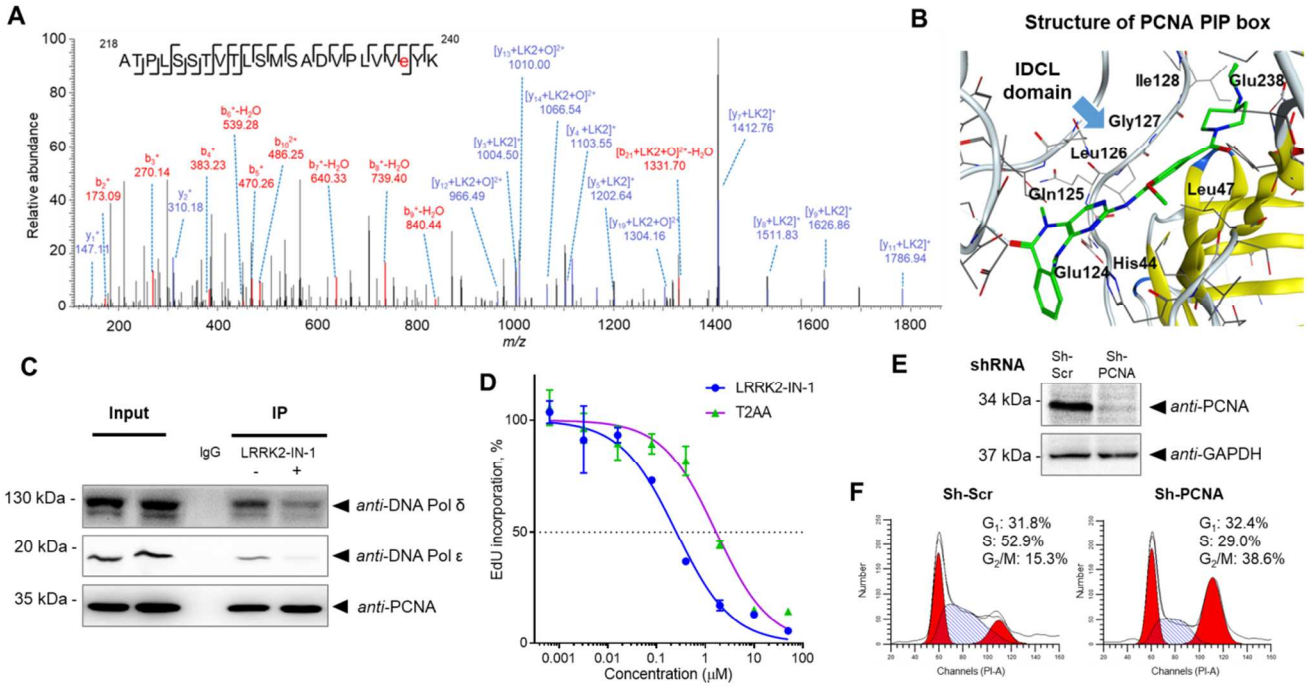
A
B
Structure of PCNA PIP box
IDCL domain
Ile128
Glu238
Gly127
Leu126
Gln125
Leu47
His44
Glu124
Relative abundance
m/z
C
Input
IP
IgG
LRRK2-IN-1
130 kDa
20 kDa
35 kDa
anti-DNA Pol δ
anti-DNA Pol ε
anti-PCNA
D
LRRK2-IN-1
T2AA
EdU incorporation, %
Concentration (μM)
E
shRNA
Sh-Scr
Sh-PCNA
34 kDa
37 kDa
anti-PCNA
anti-GAPDH
F
Sh-Scr
Sh-PCNA
G1: 31.8%
S: 52.9%
G2/M: 15.3%
G1: 32.4%
S: 29.0%
G2/M: 38.6%
Number
Channels (PI-A)

SCHEME

Scheme 1. Synthesis of LK2-P1. Reagents and conditions: (a) 1-Ethyl-3-(3-dimethylaminopropyl)carbodiimide hydrochloride (EDCI), 1-Hydroxybenzotriazole (HOBt), *N,N*-Diisopropylethylamine (DIPEA), DMF, 0°C to rt, 12 hr, 85%; (b) dicyclohexylphosphio-2',4',6'-tri-isopropylbipheny (X-Phos), tris(dibenzylidene-acetone)dipalladium ($Pd_3(bda)_3$), K_2CO_3, *t*-BuOH, 100°C, 4 hr, 40%; (c) 1. TFA, DCM, rt, 1 h, 100%; 2. 3-(but-3-yn-1-yl)-3-(2-iodoethyl)-3H-diazirine, K_2CO_3, DMF, 50°C, 12 hr, 50%.

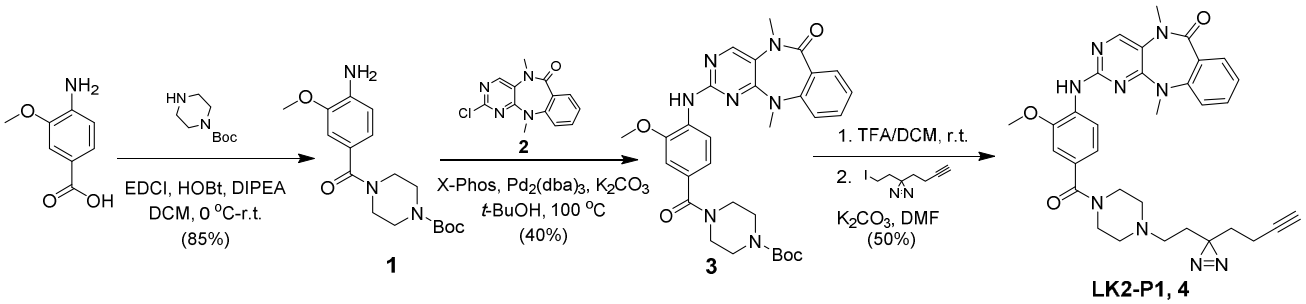

Table of Contents